FAST TRACK COMMUNICATION

Anticorrelated electrons from weak recollisions in nonsequential double ionization

J. Phys. B: At. Mol. Opt. Phys. **41** (2008) 211002 (6pp) doi:10.1088/0953-4075/41/21/211002

FAST TRACK COMMUNICATION

Anticorrelated electrons from weak recollisions in nonsequential double ionization

S L Haan, Z S Smith, K N Shomsky and P W Plantinga

Department of Physics and Astronomy, Calvin College, Grand Rapids, MI 49546, USA

E-mail: haan@calvin.edu

Received 9 September 2008, in final form 10 September 2008
Published 23 October 2008
Online at stacks.iop.org/JPhysB/41/211002

Abstract

The production of anticorrelated (back-to-back) electrons in double ionization of atoms by lasers at 483 or 800 nm is examined with 3D classical ensembles, for situations in which the energy available at recollision is less than the binding energy. Recollision excitation typically leads to unequal electron energies. The more energetic electron most often drifts into the backward direction, whereas the other electron may be more likely to drift into the forward direction. That electron often ionizes late in the first laser maximum after recollision or early in the second maximum.

(Some figures in this article are in colour only in the electronic version)

Measurements of electron and ion momenta in nonsequential double ionization (NSDI) by linearly polarized lasers indicate that very often the ionized electron pairs drift out on the same side of the atom [1–5]. Stated more mathematically, their momentum components along the laser polarization axis very often have the same sign. Accordingly, the net momentum along this polarization or longitudinal axis very often exhibits a double-peaked structure centred about zero. The correlation is also supported by theoretical models based on recollision [6], a process in which one electron departs the core but is propelled back by the oscillating laser field to share energy with the other electron. Both impact (immediate) ionization and excitation with ionization a fraction of a laser cycle later can lead to a correlated electron pair, typically drifting out in the backward direction compared with the recollision [7]. By contrast, if there is recollision excitation but the excited electron remains bound for several half-cycles of the laser field before ionizing, the correlation can be lost [8]. Thus, recollision excitation with subsequent ionization (RESI) with long time delay can fill in the doublet for long laser pulses.

Details of the net momentum spectra vary with atomic species, intensity and wavelength. For example, at lower intensities [1] or shorter wavelengths [9] the spectrum becomes a singlet rather than a doublet. Since recollisions are less energetic in these circumstances, one might expect the singlet to imply that the two ionized electrons are simply uncorrelated, with the DI process explainable through RESI. However, recent measurements [10] of individual electron momentum for low intensity actually show an anticorrelation, indicating significant probability for the electrons to drift out on the *opposite* sides of the atom. In the present paper, we employ 3D classical ensembles, primarily at wavelength $\lambda = 483$ nm and laser intensity $I = 5 \times 10^{14}$ W cm^{-2}. Our model also gives a singlet for the net longitudinal momentum spectrum and shows an anticorrelation in the individual electron momenta, as shown in figure 1. By backtracking individual trajectories, we are able to infer processes in the model that lead to the back-to-back electrons.

We employ the 3D fully classical ensemble model of [7, 11, 12]. Each ensemble typically contains one million classical atoms, each of which begins with energy of the helium ground state of -2.9035 au (we use atomic units except where explicitly noted). To prevent autoionization, we begin each run using the shielded nuclear potential $-2/\sqrt{r^2 + a^2}$, where $a = 0.825$, which is familiar from 1D studies such as [13]. Then, as in [7, 12] we change the value of a (for both electrons) after one electron reaches a predetermined distance from the nucleus, typically $r = 5$ for $\lambda = 483$ nm. We conserve energy

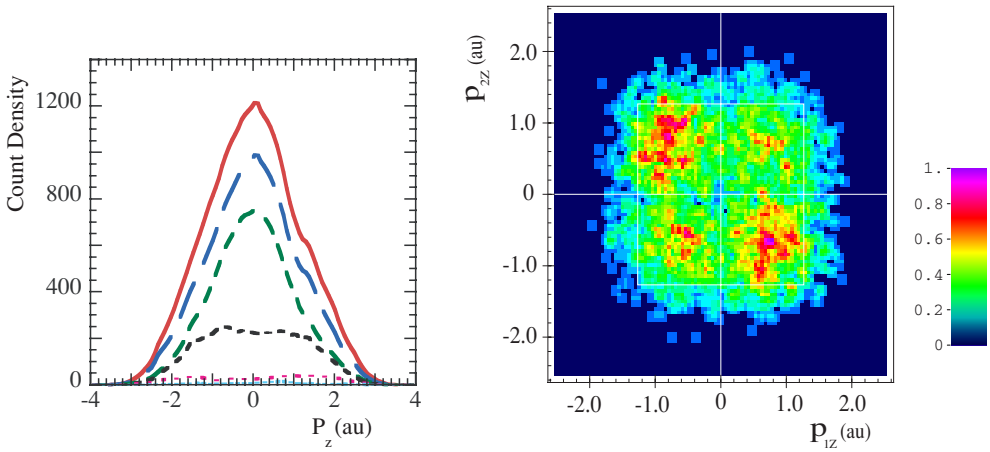

Figure 1. Left: spectrum of net or sum longitudinal (z) momentum for $I = 5 \times 10^{14}$ W cm^{-2}, $\lambda = 483$ nm. Maximum time delays δt from recollision to final ionization, from bottom to top and with progressively larger dashes, are $0.26c$ (magenta, and barely visible above tick marks), $0.50c$ (black), $1.00c$ (green) and $2.00c$ (blue). The top curve shows the full spectrum through the end of the ten-cycle pulse. The curves have been smoothed. Right: final longitudinal momentum of one electron versus the other. The plot shows an overall anticorrelation.

when we change the potential energy by giving a compensating boost in the kinetic energy for radial motion. This toggle-switch changing of a allows us to explore the importance of the nuclear force in recollision, since large-angle scattering requires a large nuclear force. Below, we analyse in detail the case of $a = 0.4$ before discussing the dependence on a. We have employed pulse lengths from 5 to 15 cycles and adjusted the distance at which we change the shielding to be sure that our results are robust. Unless indicated otherwise, results presented here will be for a ten-cycle (2+6+2) trapezoidal pulse. We use trapezoidal laser pulses because the linear turnoff does not affect the electron drift velocity.

For each doubly ionizing two-electron trajectory in the ensemble we identify the recollision time and the final ionization time, each to the nearest 0.01 cycle. We define recollision time as the time of closest approach of the two electrons after the first electron escapes the core. We define an electron to be ionized if its energy, calculated as the sum of kinetic energy plus potential energies for electron–nucleus and electron–electron interactions, becomes and subsequently remains (for at least 0.2 cycles) positive, or if the electron is outside the nuclear well[1].

For a wavelength of 780 nm and for intensities in the well-known 'knee' area of NSDI (10^{14}–10^{15} W cm^{-2}) the classical model indicated [11] that there is usually a time delay of a portion of a laser cycle between recollision and final ionization. Nonetheless, the electrons can emerge as a correlated pair [7]: an electron that is free after the recollision is likely to be swept into the backward direction (relative to the recollision direction) by the oscillating laser field, whereas an excited bound electron can be pulled back by the nucleus and escape over the barrier at the next field maximum. In [12] we used the term boomerang to describe the latter process, which is similar to what had been seen in 1D [13]. To lowest approximation, the electron's final direction of motion depends on whether it escapes before or after the field maximum, with those that escape before the maximum drifting into the backward direction.

The maximum energy available at recollision is about $3.2U_p$, where U_p is the ponderomotive energy [6]. For wavelength $\lambda = 483$ nm and intensity $I = 0.5$ PW cm^{-2}, $U_p = 0.40$, so the energy available at recollision is less than the binding energy of the positive ion (about 2 au, with some variation through the ensemble). Nonetheless, we are above the threshold for one collision to result in over-the-barrier escape. Successive curves from bottom to top in figure 1 show the net longitudinal or sum momentum parallel to the laser-polarization (z) axis for increased maximum time delay between recollision and final ionization. Trajectories with time delay up to $0.5c$ show a flat top, but for longer delays the spectrum becomes sharply peaked at zero. The singlet suggests the importance of opposite-hemisphere electrons [14]. The importance is confirmed in the right plot of figure 1, which shows the final longitudinal momentum of one DI electron versus the other. Quadrants 2 and 4 correspond to opposite-hemisphere electrons and contain 57% of the population (1969 of 3430).

A sample trajectory that leads to anticorrelated electrons is shown in figure 2. We emphasize that there is a considerable variety among trajectories, and that this one should be seen as illustrative rather than prescriptive. One electron, coded in blue, is oscillating about the fixed nucleus at the origin when the other electron, coded in red, comes in from the top and recollides. The closest approach of the electrons is marked with a pair of dots and occurs at $t = 4.54c$. After the collision we can clearly identify 'outer' and 'inner' electrons. The outer electron overshoots the core but loops around or boomerangs into the backward direction. It remains bound (by our definition) until the position shown by the arrow, when it transitions to positive energy (at $t = 4.72c$). We will show below that so far this trajectory is very typical. It also has the interesting feature of a second close encounter between the two electrons ($t = 4.76c$, and marked by the second pair of

[1] Our specific test is whether $zF_z > 0$ with $z^2 > 5$, where F denotes the net force on the electron and z the polarization direction. Also, any electron with $|z| > 10$ is declared ionized.

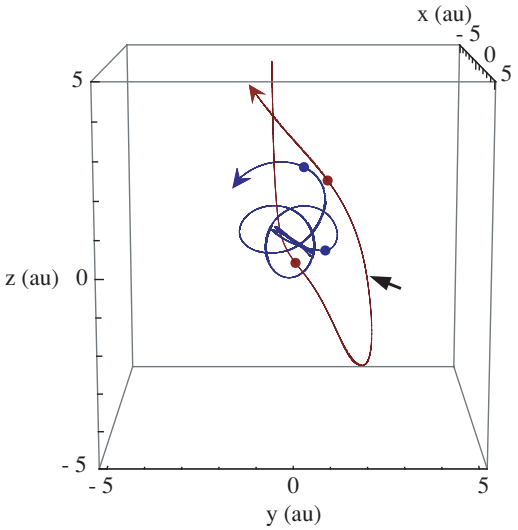

Figure 2. Sample trajectory that leads to anticorrelated electrons. One electron comes from top, collides, boomerangs and exits into the backward direction. The other electron is collisionally excited but fails to escape at the first field maximum after recollision. It escapes into the forward direction at the next field maximum, after the time interval shown. Dots show positions of closest approach for the electrons. The arrow indicates the position of the outer electron when it achieves positive energy.

dots). We end the plot as the outer electron departs the core for the final time. The inner electron continues to oscillate in the nuclear well until it escapes into the opposite $(-z)$ direction during the next barrier suppression.

We have classified the trajectories based on whether each electron is free or bound with increasing time since recollision. Results are shown in figure 3. The ascending dash-dot blue curve shows free–free population, green dashed curve shows free–bound and rapidly descending red dotted curve shows bound–bound population. The most likely recollision scenario involves the production of a short-lived doubly bound state. The two electrons escape one after the other, so the population transitions from bound–bound to bound–free to free–free. The first ionization usually occurs within a quarter cycle, almost always within a half-cycle. The solid grey curves use a slightly different definition of recollision time because if a doubly excited state is formed, closest approach could occur as the two bound electrons jostle. Thus we have also defined the recollision to occur when the electrons first come within less than 1.9 au of each other. Details of the curves depend on which definition we employ, but the main ideas do not[2]. Because the electrons ionize one after the other, we will refer to the first and second electrons to ionize as simply the first or second electron[3].

The electrons typically have different energies after the collision, as shown on the right in figure 3, where we plot the energy of the second electron versus the first at time $0.06c$ after collision[4]. Thus we have clearly identifiable inner and outer electrons, just as in our sample trajectory of figure 2. For it, the energies are $(-0.251, -0.787)$. In figure 4, we again consider longitudinal momenta, but in this plot we define the forward direction (relative to recollision) as positive and we distinguish the electrons based on the order in which they achieve final ionization. The plot shows that the first electron—plotted on the horizontal axis—most often drifts out in the backward direction, whereas the second electron is more likely to emerge in the forward direction than backward. Populations in quadrants 1–4 are 196 (6%), 1754 (51%), 1265 (37%) and 215 (6%), respectively. The white square in figure 4 shows a momentum of $\pm\sqrt{4U_p}$. We find that the first electron is more likely to achieve high longitudinal momentum. As discussed in [12], the boomerang can lead to momentum above $\sqrt{4U_p}$ at high frequency, changing the phase of the electron's oscillation relative to the laser oscillation [15] even though the electron may be bound at the time it changes direction.

We now consider the ionization of the second electron. Figure 5 shows laser phase t_i (in cycles) at the time of final ionization versus phase t_r at recollision. Same-hemisphere trajectories are included on the left and opposite-hemisphere trajectories on the right. We allow for wraparound, but to prevent ambiguity from overlap, we include only the trajectories for which the time delay between recollision and final ionization is less than 1 laser cycle. (Thus, the population considered is responsible for the green-dashed singlet in figure 1.) The absence of population along the $t_i = t_r$ diagonals reminds us that we do not have impact ionization. The same-hemisphere plot on the left shows its largest concentrations of population just before the first field maxima after collision ($t_i = 0.25$ or $0.75c$). For these trajectories, we typically have backward drifting electron pairs. The right plot of figure 5 has the corresponding clusters centred on slightly later ionization times. There is not a sharp boundary between the clusters on the respective plots, which can be explained by noting that electrons escape over the barrier with various velocities and that there may be interactions with the other electron. Electrons that do not escape in the first field maximum after recollision may escape in the second, *with escapes before the next field maximum now leading to a forward travelling electron*, opposite from the other electron and thus included in the plot on the right. This population is indicated by the clusters near $(t_r, t_i) = (0.4, 0.2)$ and $(0.9, 0.7)$. Ionizations during the subsequent waning of the field lead to the less important clusters on the left-hand plot.

The picture that emerges is as follows: there is recollision excitation, resulting most often in one loosely bound or low-energy unbound electron and one more tightly bound electron. The former boomerangs or is pushed back by the laser field and drifts out into the backward direction. The latter escapes over the barrier into either the backward (B) or forward (F) direction, depending on how many half-cycles elapse before it ionizes and whether it escapes before or after the field

[2] Similar comments apply to other plots. We have checked them all using the alternative definition of recollision time.

[3] Because of the possibility of electron exchange at recollision, this classification scheme is different from classifying recolliding versus struck electron. It is almost equivalent to classifying electrons as inner and outer, but there are trajectories in which the inner electron ionizes before the boomeranging, outer electron.

[4] This plot should not be used for estimating total energy, since both energies include e–e interaction, which would then be counted double in a sum.

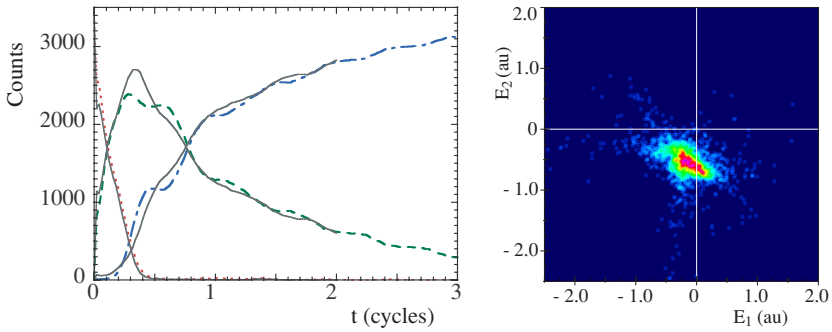

Figure 3. Left: ionization status versus time since recollision for all DI trajectories, showing shift of population from bound–bound (red-dotted) to bound–free (green dashed) to free–free (dash-dot blue). The solid grey curves extending to $t = 2c$ define recollision to occur when e–e separation drops below 1.9. Data were sampled every 0.01 cycle. Right: energy of the second electron to achieve final ionization versus the first at time $0.06c$ after recollision, showing that the electrons have unequal energies after recollision. Some trajectories are outside the region plotted.

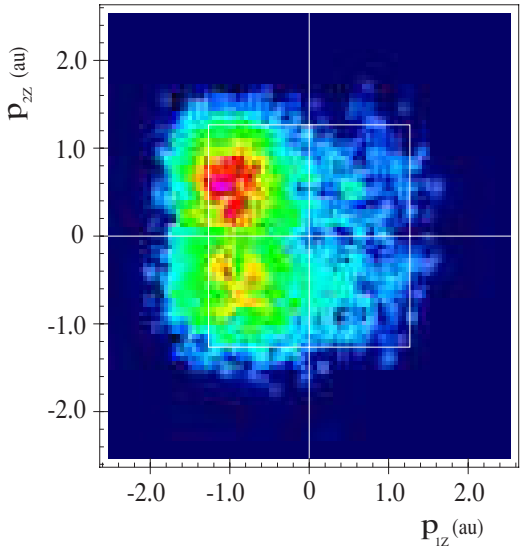

Figure 4. Final longitudinal momenta of the second electron to ionize versus the first for the same populations as in figure 1, with the forward direction defined as positive. The white square shows $\pm\sqrt{4U_p}$.

maximum. Ionization pulses for the second electron follow the sequence BF, FB, BF, FB, . . . , where commas denote pauses in the ionization due to laser zeros. Two of the first three options are F, and the total F population exceeds the total B population.

The pulses of final ionization are shown in figure 6, with solid red and dashed-blue curves for electron pairs that drift out on the same or opposite sides, respectively. Except for the few trajectories in which the first electron travels into the forward direction, the solid red peaks correspond to the B terms above and the dashed blue peaks the F terms. To generate this plot we grouped all recollision times into half-cycle bins extending from 2.1 to $2.6c$, 2.6 to $3.1c$, etc. We then determined the time interval Δt from the preceding laser zero to the final ionization for each trajectory. Thus, impact ionization would appear in $0.1c \leqslant \Delta t < 0.6c$, ionization in the first field maximum after recollision in $0.6c \leqslant \Delta t < 1.1c$, and so forth. Because of the size of the first two blue dashed peaks, the total area under the curve for the dashed blue peaks (F) will be greater than for the solid red (B). We emphasize that we classify the trajectories by the final momentum, not by the direction of motion at ionization.

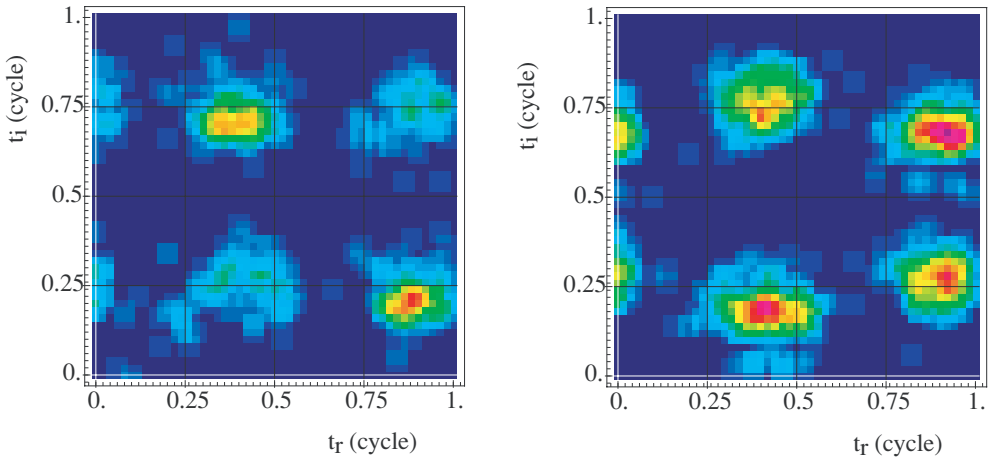

Figure 5. Final ionization phase t_i versus recollision phase t_r (both in cycles) for 483 nm, for same-hemisphere trajectories ($p_{1z}p_{2z} > 0$) on the left and opposite-hemisphere trajectories ($p_{1z}p_{2z} < 0$) on the the right. Only trajectories with a time delay of 1.0 cycle or less are included. The two plots have common colour scale, allowing direct comparison.

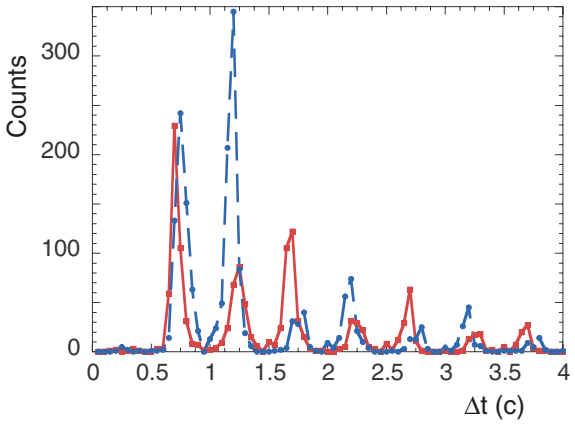

Figure 6. Pulses of ionization versus time since beginning of the half-cycle bin in which recollision occurred ($t_i - 2.0$ for collisions occurring from $2.1c$ to $2.6c$, $t_i - 2.5$ for collisions occurring from $2.6c$ to $3.1c$, and so forth). The solid red curve shows same-hemisphere (or correlated) pairs and dashed blue curve shows opposite-hemisphere (or anticorrelated) pairs. There is an initial pulse of correlated pairs, followed by two pulses of anticorrelated pairs, then a sequence of less important pulses. The overall population shows anticorrelation when the first two pulses of anticorrelated pairs are sufficiently large.

The relative heights of the first two peaks for opposite-hemisphere electrons are not as significant as might be thought at first inspection, as we have found that their relative heights depend on our operational definition of ionization. Some electrons that leave the core after the field maximum travel quite slowly and still have energy less than zero as the laser field passes through zero (and may be from say 5–10 au away from the nucleus). Our algorithm does not register 'final ionization' for these electrons until they achieve positive energy after the laser zero. An alternative definition for ionization might assign these electrons to the preceding peak. Nonetheless, by examining individual trajectories, we have identified physical reasons why the second electron can fail to ionize during the first field maximum after recollision, but succeed during the next. Sometimes the answer is simply poor timing during the first barrier suppression—the inner electron's oscillations in the well did not put it in position to escape during the time the barrier is suppressed. A second answer, though, which clearly distinguishes the first and second barrier suppressions, is the possible presence of the other electron. For example, the first electron, which overshot the core but was pulled back, can raise the barrier slightly at a critical time so the second electron fails to escape during that field maximum. This is what happens in the sample trajectory of figure 2. By the next barrier suppression, the first electron no longer has an effect, and the second electron escapes easily, usually before the field maximum and thus into the forward direction.

We have also investigated the DI for the longer wavelength 800 nm and for intensity 2.0×10^{14} W cm^{-2}, again slightly above the threshold for having a single recollision lead to over-the-barrier escape. We again find anticorrelation, and for the same reasons as for 483 nm. Results are shown in figure 7. In addition, we have investigated final ionization for various values of the final shielding parameter. We have found that for small shielding, the recollisions become less effective, the average time delay between recollision and final ionization increases and the anticorrelation is lost.

Finally, we have recently considered a case in which one recollision is insufficient for subsequent over-the-barrier ionization. In particular, we have considered $\lambda = 483$ nm and $I = 3 \times 10^{14}$ W cm^{-2}, which reduces U_p to 0.24. To compensate for the large drop in DI yield, we increased our ensemble size to 12 million. Our results do not show significant anticorrelation (779 of 1520 or 51% are forward–back combinations) for a 10-cycle pulse. An investigation of individual trajectories indicates multiple collisions. These may be separated by one or more full cycles, but we have identified two critical times in the trajectories when additional (though weak) collisions are most likely. One possibility occurs during initial ionization, as one electron may become loosely bound on one side of the atom and traverse the core on its way out, transferring some energy to the other electron. A second possibility is to have 'double collisions' similar to the trajectory shown in figure 2 for the higher intensity. In some trajectories both electrons escape at low speed when the barrier is maximally suppressed. For such escapes, a small difference in velocity or escape time can influence the final drift direction. We will present a more detailed analysis elsewhere.

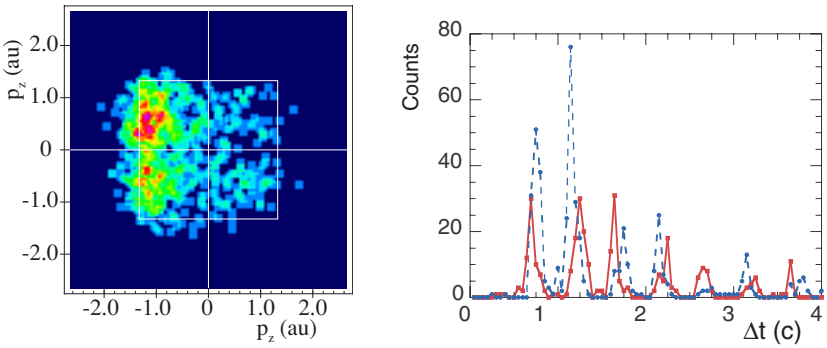

Figure 7. For $\lambda = 800$ nm, $I = 0.2$ PW cm^{-2}. Left: final longitudinal momenta of the second electron to ionize versus the first, with the forward direction defined as positive. Right: pulses of same-hemisphere (solid red) and opposite-hemisphere (dashed blue) ionizations as in figure 6.

In conclusion, we have seen that in our classical model, decreasing the laser wavelength or intensity can lead from having overall electron correlation to having an overall anticorrelation in the electron momenta parallel to laser polarization. We have found that after recollision the more energetic electron typically boomerangs or is pushed into the backward direction by the laser field. The second electron might ionize before (approximately) the first field maximum after recollision and also drift into the backward direction. If it escapes after the field maximum or in the second maximum after recollision, it is likely to drift into the forward direction. We have also noted that when the first electron boomerangs, it may re-encounter the other electron and influence its ionization. We showed an example in which the re-encounter delayed the ionization of the second electron, but there is also the possibility for a second albeit weak collision that helps to ionize the second electron. This double collision process is apparently especially important if the intensity is below the threshold for one-collision excitation with subsequent ionization.

Acknowledgments

This material is based upon the work supported by the National Science Foundation under grant no 0653526 to Calvin College. We also acknowledge our ongoing collaboration with J H Eberly's Group at the University of Rochester.

References

[1] Weber Th *et al* 2000 *Phys. Rev. Lett.* **84** 443
[2] Moshammer R *et al* 2000 *Phys. Rev. Lett.* **84** 447
[3] Eremina E *et al* 2003 *J. Phys. B: At. Mol. Opt. Phys.* **36** 3269
[4] For reviews, see Dörner R, Weber Th, Weckenbrock M, Staudte A, Hattass M, Schmidt-Böcking H, Moshammer R and Ullrich J 2002 *Adv. At. Mol. Opt. Phys.* **48** 1
Ulrich J, Moshammer R, Dorn A, Dörner R, Schmidt L Ph H and Schmidt-Böcking H 2003 *Rep. Prog. Phys.* **66** 1463
Becker and A, Dörner R and Moshammer R 2005 *J. Phys. B: At. Mol. Opt. Phys.* **38** S753–72
[5] For a review article regarding the use of many-body S-matrix theory in intense fields see Becker A and Faisal F H M 2005 *J. Phys. B : At. Mol. Opt. Phys.* **38** R1–R56
[6] Corkum P B 1993 *Phys. Rev. Lett.* **71** 1994
Schafer K J, Yang B, DiMauro L F and Kulander K C 1993 *Phys. Rev. Lett.* **70** 1599–602
See also Kulander K C, Schafer K J and Krause J L 1995 *Super Intense Laser-Atom Physics* ed B Piraux, A L'Huillier and K Rzazewski (New York: Plenum) p 95
[7] Haan S L, Smith Z S and VanDyke J S 2008 *Phys. Rev. Lett.* **101** 113001
[8] deJesus V L B, Feuerstein B, Zrost K, Fischer D, Rudenko A, Afaneh F, Schröter C D, Moshammer R and Ullrich J 2004 *J. Phys. B: At. Mol. Opt. Phys.* **37** L161
[9] Alnaser A S, Comtois D, Hasan A T, Villeneuve D M, Kieffer J-C and Litvinyuk I V 2008 *J. Phys. B: At. Mol. Phys.* **41** 031001
[10] Liu Y, Tschuch S, Rudenko A, Dürr M, Siegel M, Morgner U, Moshammer R and Ullrich J 2008 *Phys. Rev. Lett.* **101** 053001
[11] Haan S L, Breen L, Karim A and Eberly J H 2006 *Phys. Rev. Lett.* **97** 103008
Haan S L, Breen L, Karim A and Eberly J H 2007 *Opt. Exp.* **15** 767
[12] Haan S L and Smith Z S 2007 *Phys. Rev.* A **76** 053412
[13] Panfili R, Haan S L and Eberly J H 2002 *Phys. Rev. Lett.* **89** 113001
[14] Ho P J 2005 *Phys. Rev.* A **72** 045401
[15] Paulus G G, Becker W, Nicklich W and Walther H 1994 *J. Phys. B: At. Mol. Opt. Phys.* **27** L703
Walker B, Sheehy B, Kulander K C and DiMauro L F 1996 *Phys. Rev. Lett.* **77** 5031